Hepatocellular Carcinoma Diagnosis by Detecting α-Fucosidase with a Silicon Nanowire Field-Effect Transistor Biosensor

Chao-Yu Yang,[1,=] **Hsu-Cheng Chiang,**[1,=] **Chia-Jung Kuo,**[1] **Chia-Wei Hsu,**[1] **Shih-Feng Chan,**[2] **Zong-Yan Lin,**[2] **Chun-Hung Lin,**[2,z] **and Yit-Tsong Chen** ⓘ [1,3,z]

[1]*Department of Chemistry, National Taiwan University, Taipei 106, Taiwan*
[2]*Institute of Biological Chemistry, Academia Sinica, Nankang, Taipei 115, Taiwan*
[3]*Institute of Atomic and Molecular Sciences, Academia Sinica, Taipei 106, Taiwan*

Hepatocellular carcinoma (HCC) is one of the most frequent and fatal cancers. However, traditional clinical imaging modalities cannot detect small tumors and are not suitable for the early stage diagnosis of hepatic cancer. In this study, we applied silicon nanowire field-effect transistors (SiNW-FETs) as a biosensor to detect α-fucosidase (AFU), which is a biomarker of high sensitivity and specificity for the HCC diagnosis. Fuconojirimycin (FNJ) is an inhibitor of AFU with very high binding affinity to AFU. By modifying the FNJs of optimized receptor length and number density on SiNW-FET (referred to as FNJ/SiNW-FET), this biosensing device can detect AFU to a very low concentration level with the detection limit of ∼1.3 pM. With the merits of high sensitivity, target specificity, and label-free detection, this FNJ/SiNW-FET can be developed as a powerful biosensor to detect AFU for the early HCC diagnosis.

Hepatic cancer, known as a common cancer, is one of the leading causes of mortality. Hepatocellular carcinoma (HCC) is the most frequent hepatic cancer and accounts for the approximately 90% of all primary liver cancers. The high fatality rate of HCC arises from a lack of the diagnostic accuracy in early detection. Therefore, the early diagnosis plays an important role to raise the clinical cure rate. To date, many clinical imaging modalities have been used for the diagnosis of hepatic cancer; however, these imaging methods cannot detect small tumors and are not suitable for the early stage cancer detection.

It has been known that α-fucosidase (AFU) could be a tumor marker with high sensitivity and specificity for HCC diagnosis.[1] AFU is an enzyme catalyzing the hydrolytic removal of L-fucose residues that are mainly attached to the non-reducing terminus of glycan chains.[2] Fucose-containing glycoconjugates are associated with a myriad of important pathological events. The aberrant presence of serum AFU has been associated with HCC, which makes AFU a prospective tumor marker in the early detection of HCC.[3] In addition, increasing attention has been drawn to the potent inhibitors of AFU. Fuconojirimycin (FNJ), first synthesized by Fleet et al.,[4] is one of the strongest AFU inhibitors with very high affinity. FNJ and its derivatives have the dissociation constants (K_d) of the AFU-FNJ complexes in the range of $10^{-8}-10^{-11}$ M.[2,5,6] As a rival to fucose in association with AFU, FNJ has a similar chemical structure to fucose (Figure 1A) and competes against fucose for binding with AFU.

Silicon nanowire field-effect transistors (SiNW-FETs)-based electrical biosensors have aroused tremendous interest in the past decades for biomedical applications. With the advantages of high sensitivity, target selectivity, real-time measurement, and label-free detection, SiNW-FETs have been widely used as an efficient and versatile platform[7] for the detections of ions,[8] small molecules,[9] proteins,[10,11] and other biomolecules.[12,13] A SiNW has a large surface-to-volume ratio, which enables a slight external electric field to modulate the electrical conductance significantly inside a SiNW-FET. When modified with selected receptors (probing molecules) on the SiNW surface, the SiNW-FET can be used as a biosensor to detect specific targets in real time with sensitive, label-free sensing ability. As illustrated in Figure 1B, a SiNW-FET device is composed of a conducting channel of semiconductive SiNWs together with the source, drain, and gate electrodes, where the SiNW channel is located between the source and drain electrodes. In biosensing experiments, an Ag/AgCl reference electrode, acting as a solution gate electrode, is immersed in the sample solution and can be used to apply various gate voltages or kept at ground potential to reduce electrical noise during the biosensing measurements.

In this study, we demonstrate that a SiNW-FET can be an ultra-sensitive biosensor for AFU detection by modifying FNJ on the SiNW surface (referred to as an FNJ/SiNW-FET device) for the specific and label-free detection of AFU. By applying an FNJ/SiNW-FET to detect AFU, the distinctive electrical responses of the FNJ/SiNW-FET to various concentrations of AFU (denoted by C_{AFU}) can be used to determine the K_d value of the AFU-FNJ complex. To find the best device sensitivity of an FNJ/SiNW-FET for detecting AFU, we optimized the surface-modification of the FNJ/SiNW-FET by adjusting the receptor length and number density of the FNJ to be modified on SiNW-FET. As displayed in Figures 1C−1F, four FNJ derivatives of different lengths were used to test their binding strengths with AFU. These FNJ derivatives contain the core structure of FNJ (represented by red color in Figures 1C−1F) to mimic the transition state of the AFU-catalyzed reaction[14] and an extended amino group attached to a three-, six- or nine-carbon linker. We additionally optimized the number density of FNJ receptors to be modified on SiNW-FET to achieve the best detection sensitivity for AFU.

Complementary to the SiNW-FET experiments, we also conducted molecular docking simulation to calculate the optimal binding structure of the AFU-FNJ complex. The molecular docking simulation attempted to compute the noncovalent binding of a macromolecule and a small molecule, starting with their unbounded structures,[15] and have been widely applied for drug screening and pharmaceutical designs. In this study, we calculated the molecular docking of FNJ-based receptors (regarded as flexible ligands) into the binding site of AFU (regarded as a fixed macromolecule) to optimize their binding strengths. Assisted with the molecular docking computation, this novel nanobiosensing methodology of using a highly sensitive FNJ/SiNW-FET for the label-free detection of AFU can be developed as a powerful tool for the early HCC diagnosis.

=These authors contributed equally to this work.
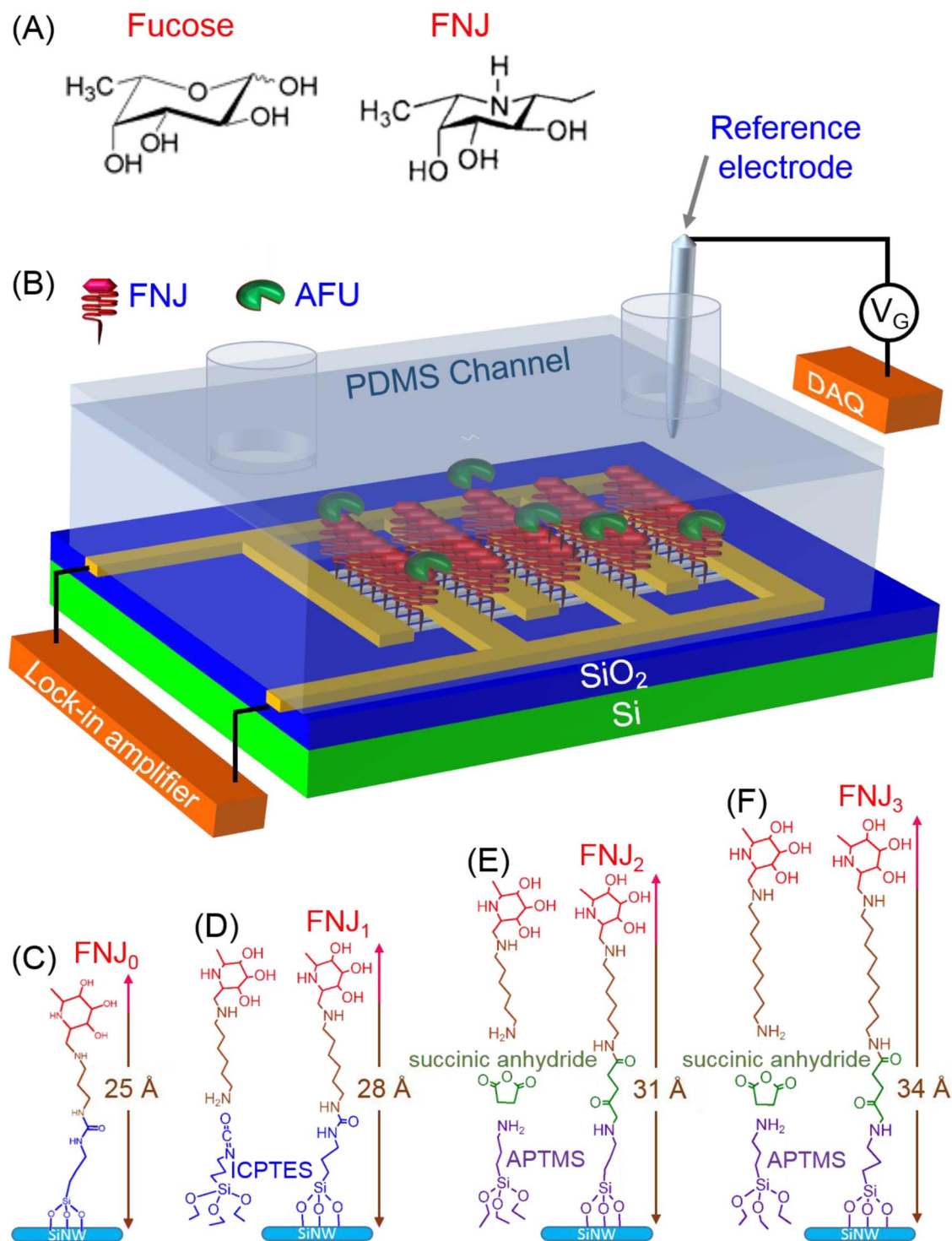zE-mail: chunhung@gate.sinica.edu.tw; ytcchem@ntu.edu.tw

Figure 1. (A) The chemical structures of fucose and FNJ show their structural similarity. As a rival to fucose, FNJ competes with fucose for binding with AFU. (B) A schematic illustration of an MPC SiNW-FET biosensor. A PDMS microfluidic channel was coupled with an FNJ/SiNW-FET for the delivery of sample solution. The solution-gate voltage (V_G) was applied through an Ag/AgCl electrode and the source-drain current (I_{SD}) was detected with a lock-in amplifier at the modulation frequency of 79 Hz, time constant of 100 ms, and V_{SD} of 5 mV. (C−F) Four FNJ derivatives with different lengths of (C) 25 Å (FNJ_0), (D) 28 Å (FNJ_1), (E) 31 Å (FNJ_2), and (F) 34 Å (FNJ_3) were modified on MPC SiNW-FETs to test the binding affinity to AFU. Each FNJ receptor includes the core structure of FNJ (represented by red color) and the elongated linker (drawn by brown, green, and blue colors). The drawing is not to scale.

Experimental

The preparation of recombinant AFU, including protein overexpression and purification, was carried out according to the previous report.[6] The syntheses of the three FNJ derivatives from L-gulono-1,4-lactone were modified on the basis of a reported procedure.[14]

The SiNW-FET devices were fabricated following a standard photolithography process, of which the detailed procedures can be found in our previous work.[12,16] Briefly, the boron-doped (B:Si = 1:4000) SiNWs were synthesized catalytically with 20 nm gold nanoparticles via chemical vapor deposition (CVD) reaction (460°C for

12.5 min)[17] and then transferred to a Si wafer (i.e., a SiO_2/Si substrate) with a contact printing method.[18] Multiple-parallel-connected (MPC) SiNW-FETs, as illustrated schematically in Figure 1B, were fabricated with several tens of p-type SiNWs connected by two sets of interdigitated source and drain electrodes. The metal leads of Ni (70 nm thick) and Al (100 nm thick) were patterned by photolithography and deposited with a thermal evaporator. The surface of the Al layer was later oxidized to form an Al_2O_3 film of several nanometers thick, serving as an insulation coat to prevent electric leakage during biosensing experiments. The MPC SiNW-FETs are crucial for recognizing weakly charged species or trace amounts of analytes, because of their higher sensitivity and reliability than traditional SiNW-FETs with only single or a few SiNWs as a conducting channel.[16]

To optimize the AFU-FNJ interaction, we examined various receptor lengths and number densities of FNJ to be modified on an MPC SiNW-FET. As shown in Figures 1D−1F, three FNJ-based receptors were experimentally tested with their lengths of 28 Å (denoted by FNJ_1), 31 Å (FNJ_2), and 34 Å (FNJ_3). In the modification of the FNJ derivatives, 3-isocyanatopropyl-triethoxysilane (ICPTES) or 3-aminopropyl-trimethoxysilane (APTMS) was first modified on an MPC SiNW-FET (to form an ICPTES/SiNW-FET Figure 1D, or an APTMS/SiNW-FET, Figures 1E−1F), the FNJ derivatives were then immobilized on ICPES/SiNW-FET or APTMS/SiNW-FET via their terminal amino groups to react with the cyanato group of ICPTES by nucleophilic addition (Figure 1D) or to link the amino group of APTMS via a succinic anhydride by carbodiimide crosslinking (Figures 1E−1F).

Similarly, the number density of FNJ was also optimized to be modified on an MPC SiNW-FET to gain the best detection sensitivity. Since FNJ_1 has the strongest binding with AFU among the FNJ_n (n = 1, 2, and 3) in the receptor length test, we chose an FHJ_1/SiNW-FET for testing the number density of FNJ_1. Different densities of FNJ_1 were modified on an MPC SiNW-FET by mixing 5% of ICPTES with propyl-trimethoxysilane (PTMS) at the ratios of 1:0, 1:1, 1:4, 1:10, and 1:20. PTMS was inactive to react with the FNJ derivative but could act as a spacer to dilute the FNJ_1 in the surface modification of SiNW-FET and to avoid the interference (e.g., steric hindrance) from neighboring FNJ_1s in biosensing measurements.

In the electrical measurements with SiNW-FETs, the output curves (i.e., source-drain current (I_{SD}) vs. bias voltage (V_{SD}) curves, or represented by $I_{SD}-V_{SD}$ plots) were acquired with a lock-in amplifier (Signal Recovery, 7265 DSP) at the modulation frequency of 79 Hz, time constant of 100 ms, and V_{SD} of 5 mV (as displayed in Figure 1B). A solution-gate voltage (V_G) was applied from a power supply (Keithley, 2400 Source Meter) or a data acquisition (DAQ) system through an Ag/AgCl electrode to obtain the transfer curves (i.e., $I_{SD}-V_G$ plots). In consideration of the Debye-Hückel screening effect in the FET-based biosensing measurements, AFU was dissolved in 0.01 × phosphate-buffered saline (PBS, composed of 1.37 mM NaCl, 27 μM KCl, 100 μM Na_2HPO_4, 20 μM KH_2PO_4 in NaOH at pH 9, with the Debye-Hückel length of 7.4 nm) in all of the measurements throughout this study. The SiNW-FET device was coupled with a polydimethylsiloxane (PDMS) microfluidic channel (L 6.26 mm × W 500 μm × H 50 μm), through which a sample solution was delivered at the flow rate of 7 μL/min driven by a syringe pump (Figure 1B).

To calculate the FNJ-AFU interaction, a software of molecular docking simulation of AutoDock was used to compute the binding conformations and energies between AFU and different FNJ_n (n = 0, 1, 2, and 3)-based receptors (Figures 1C−1F). During the simulation, AFU was set as a macromolecule of a fixed structure and FNJ_n (n = 0, 1, 2, and 3) with various lengths were set as ligands to interact with AFU (with an initial position of 4 nm away from AFU). MGLTools was also employed to visualize and analyze the simulation results.

Results and Discussion

In Figure 2A, the molecular docking simulation reveals the inhomogeneous electrical potential distribution on the AFU surface,

on which the lowest potential is centered around the concave AFU surface. Moreover, a comparison of the surface potential mapping with the binding structure of an experimental X-ray crystal structure of AFU-fucose complex (PDB code: 1ODU)[19] manifests that the concave AFU surface is colocalized with the binding site of the AFU-fucose complex. In Figure 2B, the simulations of fucose, FNJ_1, FNJ_2, and FNJ_3 (represented by brown, blue, orange, and green lines, respectively) reveal that the locations of the docked fucose or FNJ_n (n = 1, 2, and 3) with AFU are almost the same as that of the experimental AFU-fucose crystal (the pink line in Figure 2B). These computational results confirm the reliability of the molecular docking simulation, indicating that the core structures of FNJ_n (n = 1, 2, and 3) have tight and specific bindings with AFU and the amino acid residues of AFU are responsible for the AFU-FNJ_n binding. While the core structures of FNJ_n (n = 1, 2, and 3) bind to AFU have no significant difference, the interactions between AFU and the elongated linkers of FNJ_n are different. According to the calculation by PyMOL (an open-source software created by Warren Lyford DeLano for molecular visualization), the optimal depth of the concave AFU surface to accommodate the core structure of FNJ is about 28 Å, suggesting that FNJ_1 (28 Å) has an appropriate length for strong binding with AFU. In the molecular docking simulation, we also tested a shorter receptor length of 25 Å (represented as FNJ_0, Figure 1C) by reducing three methylene groups of FNJ_1. Figure 2C shows the calculated binding of FNJ_0 to AFU, where the receptor length is too short to colocalize the core structure of FNJ_0 with the binding site of AFU, resulting in a nonspecific binding. The calculated binding energies of FNJ_n (n = 0, 1, 2, and 3) with AFU are listed in Table I, in which the optimal receptor length (28 Å) of FNJ_1 gains the maximal interaction with AFU, yielding the binding energy of −6.1 kcal/mol. In comparison, the core structure of FNJ with a shorter (FNJ_0) or longer (FNJ_2 and FNJ_3) receptor length does not reach an optimal interaction with AFU, resulting in a less stable associated complex with smaller binding energy. These docking simulations suggest that a proper receptor length is crucial for the stable binding.

Assisted with the molecular docking simulation, we modified FNJ_n (n = 1, 2, or 3) on an MPC SiNW-FET to form an FNJ_n/SiNW-FET for experimentally testing its detection ability of AFU. The biosensing detection of AFU with an FNJ_n/SiNW-FET was conducted by measuring the transfer curves (i.e., $I_{SD}-V_G$ plots) as a function of C_{AFU}, of which the standard experimental procedures can be found in our previous publications.[7,16] By fitting the experimental data points of the measured transfer curves to the Langmüir adsorption isotherm model,[16] the K_d value of the AFU-FNJ_n (n = 1, 2, or 3) complex was determined as listed in Table I. It is interesting to note that the determine K_d value increases with the increasing receptor length. Among the FNJ_n tested, FNJ_1 has the strongest binding with AFU, which is consistent with the computed results of molecular docking simulation.

To gain the device sensitivity of an FNJ_n/SiNW-FET for detecting AFU, we also optimize the number density of FNJ_n (n = 1, 2, or 3) on the FNJ_n/SiNW-FET. Since FNJ_1 has the strongest binding affinity to AFU, we employed an FNJ_1/SiNW-FET as a testing device to be modified with different number densities of FNJ_1. In the surface modification of FNJ_1, we started with a mixture of ICPTES:PTMS = 1:0, 1:1, 1:4, 1:10, and 1:20, respectively, to be immobilized on an MPC SiNW-FET. The subsequent modification procedures are described earlier in the Experimental section. As aforementioned, PTMS is inactive to react with FNJ_1 but could serve as a spacer to dilute the density of FNJ_1 on the SiNW-FET and to avoid the interference (e.g., steric hindrance) from neighboring FNJ_1s in biosensing measurements. The determined K_d values of the AFU-FNJ_1 complexes with different number densities of FNJ_1 on SiNW-FET are listed in Table I, where an FNJ_1/SiNW-FET of FNJ_1:PTMS = 1:4 on the SiNW surface possesses the strongest binding affinity to AFU.

After the optimizations of receptor length (28 Å) and number density (FNJ_1:PTMS = 1:4) of FNJ_1 on the FNJ_1/SiNW-FET, we employed this optimal biosensing device for the label-free and real-time detections of AFU. Figure 3A shows the measured $I_{SD}-V_G$ curves of
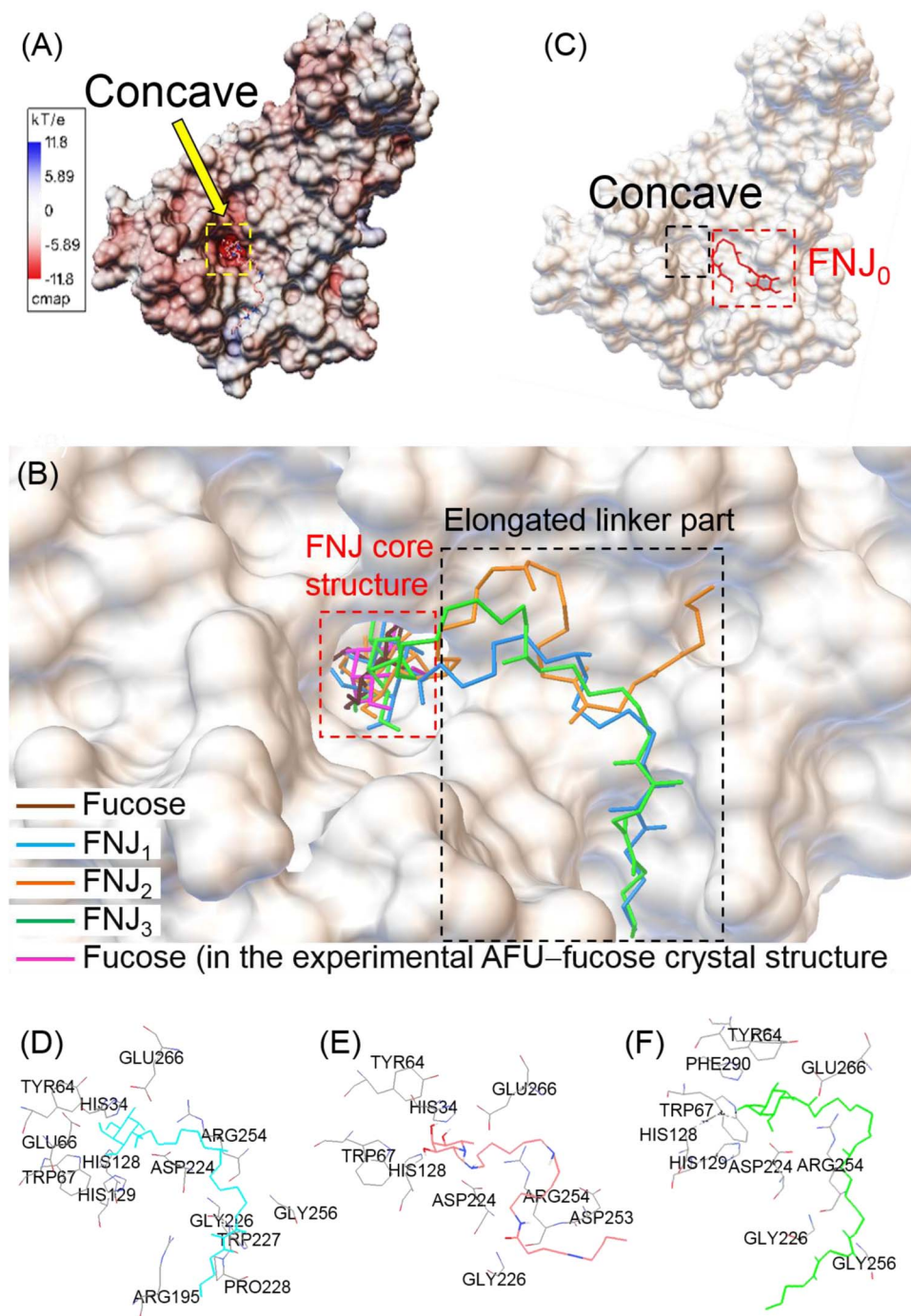
Figure 2. (A) The surface potential mapping of AFU was performed with AutoDock simulation and MGLTools analysis, revealing that the lowest potential is centered around the concave AFU surface (i.e., the binding site). (B) The molecular docking simulations show that the location of the docked fucose (brown), FNJ_1 (blue), FNJ_2 (orange), or FNJ_3 (green) with AFU is almost the same as that of the experimental AFU-fucose crystal (pink), but the positions of the elongated linkers are different. (C) The molecular docking simulation for the FNJ_0 receptor (25 Å in length) shows that the core structure of FNJ_0 fails to bind the concave AFU surface (i.e., the binding site), resulting in nonspecific binding with AFU. (D−F) The interaction analyses between AFU and (D) FNJ_1, (E) FNJ_2, and (F) FNJ_3 show that the residues of AFU are responsible for the AFU-FNJ interaction.

the FNJ_1/SiNW-FET in response to various $C_{AFU} = 0−1$ nM. Since AFU (pI ∼ 6, estimated theoretically from the amino acid sequence of AFU) is negatively charged in $0.01 \times$ PBS at pH 9, the capture of AFU by FNJ_1/SiNW-FET induced more charge carriers (holes) in the p-type SiNW-FET due to a gating effect, consequently resulting in the increase of the channel current (I_{SD}) and the upward shift of the transfer curve upon adding more C_{AFU}. As a standard procedure to avoid device-to-device variation, we converted the current change caused

by AFU-FNJ binding (ΔI_{SD} at $V_G = −0.45$ V in Figure 3A, relative to the buffer solution) to the corresponding change in V_G (ΔV_G^{cal} in Figure 3A, termed the "calibrated response") from the transfer curves ($I_{SD}−V_G$) of the FET device used.[16,20] As plotted in Figure 3B, the normalized response ($\Delta V_G^{cal}/\Delta V_{G,max}^{cal}$) increased as the C_{AFU} rose, which then reached a plateau at $C_{AFU} > 200$ pM (i.e., the saturated ΔV_G^{cal} and denoted by $\Delta V_{G,max}^{cal}$). To calculate the binding affinity of FNJ_1/SiNW-FET against AFU, we plotted the $C_{AFU}/\Delta V_G^{cal}$ vs. C_{AFU}

Table I. Optimizations of the receptor length and number density of the FNJ derivatives to be modified on an MPC SiNW-FET for the sensitive detection of AFU.

	Receptor condition	Experimentally measured K_d value	Theoretically computed binding energy
Receptor length	FNJ$_0$ (25 Å)		−4.5 kcal/mol
	FNJ$_1$ (28 Å)	8.8 ± 4.3 pM	−6.1 kcal/mol
	FNJ$_2$ (31 Å)	96.8 ± 1.4 pM	−5.7 kcal/mol
	FNJ$_3$ (34 Å)	258 ± 3 pM	−5.5 kcal/mol
	FNJ$_1$:PTMS		
	1:0	24.4 ± 2.6 pM	
	1:1	12.8 ± 2.2 pM	
Number density ratio	1:4	8.8 ± 4.3 pM	
	1:10	14.4 ± 3.0 pM	
	1:20	14.4 ± 1.3 pM	

curve (in the inset of Figure 3B) and determined the $K_d = 8.8 \pm 4.3$ pM of the AFU-FNJ complex by a least-squares fit to the Langmüir adsorption isotherm model.
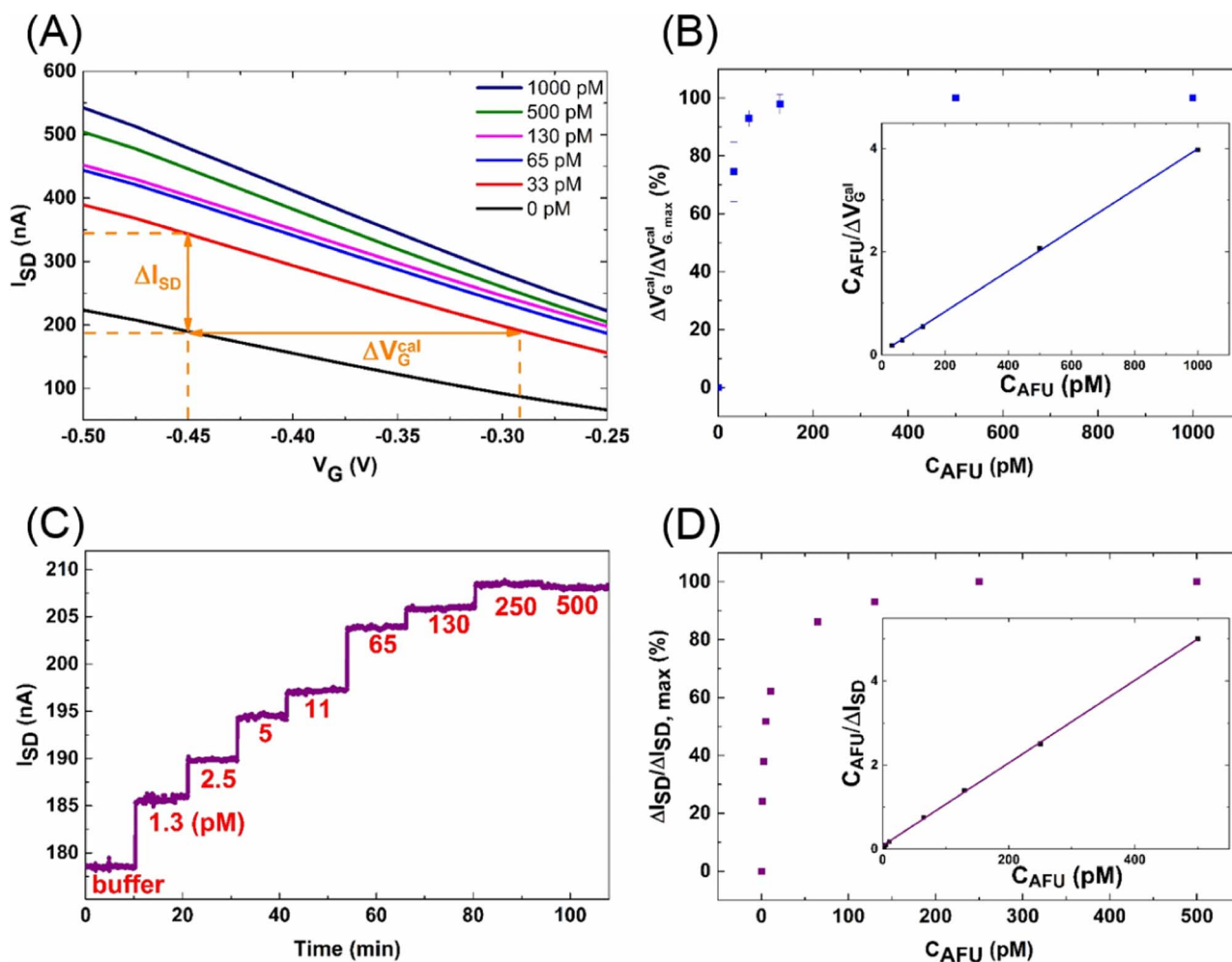
Figure 3C shows the real-time measurement of an FNJ$_1$/SiNW-FET in response to various $C_{AFU} = 0-500$ pM, in which the observable current change (ΔI_{SD}) demonstrates that this FNJ$_1$/SiNW-FET possesses the limit of detection (LOD) of $C_{AFU} \sim 1$ pM and was saturated at $C_{AFU} > 250$ pM (denoted by $\Delta I_{SD, max}$). With these experimental data of the real-time measurements (Figure 3C), the normalized current change ($\Delta I_{SD}/\Delta I_{SD, max}$) vs. C_{AFU} plot is displayed in Figure 3D. As shown in the inset of Figure 3D, $K_d = 5.0 \pm 0.5$ pM of the AFU-FNJ complex was also obtained from these real-time measurements by a least-squares fit to the Langmüir adsorption isotherm model. The similar K_d values determined from both transfer curves and real-time measurements by FNJ$_1$/SiNW-FET manifest the fidelity of the electrical measurements with this novel nanobiosensing gadget.

Summary

In this work, SiNW-FETs have been modified with FNJ-based receptors of the optimized receptor length and number density for sensitively detecting AFU. The FNJ$_1$ of 28 Å in length was determined experimentally to be proper for the core structure of FNJ to interact with AFU, which is consistent with the computational results by molecular docking simulation. The number density of FNJ$_1$:PTMS

Figure 3. (A) The transfer curves (i.e., I$_{SD}$–V$_G$ plots) of an FNJ$_1$/SiNW-FET were measured in response to various $C_{AFU} = 0-1$ nM. (B) The normalized $\triangle V_G/\triangle V_{G, max}$ vs. C_{AFU} data points are converted from the I$_{SD}$–V$_G$ curves in (A). The inset shows $K_d = 8.8 \pm 4.3$ pM for the AFU-FNJ$_1$ complex was determined from the $C_{AFU}/\Delta V_G^{cal}$ vs. C_{AFU} plot by a least-squares fit to the Langmüir adsorption isotherm model. (C) The real-time measurement of an FNJ$_1$/SiNW-FET as a function of $C_{AFU} = 0-500$ pM with an LOD of 1.3 pM. (D) The normalized $\Delta I_{SD}/\Delta I_{SD, max}$ vs. C_{AFU} plot is converted from the real-time measurement in (C). The inset shows a least-squares fit of the $C_{AFU}/\Delta I_{SD}$ vs. C_{AFU} plot to the Langmüir adsorption isotherm model, yielding $K_d = 5.0 \pm 0.5$ pM for the AFU-FNJ$_1$ complex.

= 1:4 modified on an MPC SiNW-FET could reach the best detection sensitivity for AFU. With these optimal modifications, an FNJ_1/SiNW-FET was employed to detect AFU with the LOD of $C_{AFU} = 1.3$ pM and the K_d value of the AFU-FNJ complex was determined to be 8.8 ± 4.3 pM (or 5.0 ± 0.5 pM) by the transfer curve (or real-time) measurements. With the high sensitivity and label-free detection of an FNJ/SiNW-FET, this nanobiosensing methodology for AFU detection can be developed as a powerful tool for the early HCC diagnosis.

Acknowledgments

ORCID

Yit-Tsong Chen ⓘ https://orcid.org/0000-0002-6204-8320

References

1. M. G. Giardina, M. Matarazzo, A. Varriale, R. Morante, A. Napoli, and R. Martino, *Cancer*, **70**, 1044 (1992).
2. Z. Tu, Y. N. Lin, and C. H. Lin, *Chem. Soc. Rev.*, **42**, 4459 (2013).
3. M. G. Giardina, M. Matarazzo, R. Morante, A. Lucariello, A. Varriale, V. Guardasole, and G. DeMarco, *Cancer*, **83**, 2468 (1998).
4. G. W. J. Fleet, S. K. Namgoong, C. Barker, S. Baines, G. S. Jacob, and B. Winchester, *Tetrahedron Lett.*, **30**, 4439 (1989).
5. C. F. Chang, C. W. Ho, C. Y. Wu, T. A. Chao, C. H. Wong, and C. H. Lin, *Chem. Biol.*, **11**, 1301 (2004).
6. C. W. Ho, Y. N. Lin, C. F. Chang, S. T. Li, Y. T. Wu, C. Y. Wu, C. F. Chang, S. W. Liu, Y. K. Li, and C. H. Lin, *Biochemistry*, (2006), 5695.
7. B.-R. Li, C.-C. Chen, U. R. Kumar, and Y.-T. Chen, *Analyst*, **139**, 1589 (2014).
8. A. Anand, C. R. Liu, A. C. Chou, W. H. Hsu, R. K. Ulaganathan, Y. C. Lin, C. A. Dai, F. G. Tseng, C. Y. Pan, and Y. T. Chen, *ACS Sensors*, **2**, 69 (2017).
9. S. Banerjee, Y. J. Hsieh, C. R. Liu, N. H. Yeh, H. H. Hung, Y. S. Lai, A. C. Chou, Y. T. Chen, and C. Y. Pan, *Small*, **12**, 5524 (2016).
10. Y. Cui, Q. Wei, H. Park, and C. M. Lieber, *Science*, **293**, 1289 (2001).
11. S. P. Lin, C. Y. Pan, K. C. Tseng, M. C. Lin, C. D. Chen, C. C. Tsai, S. H. Yu, Y. C. Sun, T. W. Lin, and Y. T. Chen, *Nano Today*, **4**, 235 (2009).
12. K. I. Chen, B. R. Li, and Y. T. Chen, *Nano Today.* (2011), 131.
13. A. Zhang and C. M. Lieber, *Chem. Rev.*, **116**, 215 (2016).
14. C. Y. Wu, C. F. Chang, J. S. Y. Chen, C. H. Wong, and C. H. Lin, *Angew. Chemie - Int. Ed.*, **42**, 4661 (2003).
15. O. Trott and A. J. Olson, *J. Comput. Chem.*, **31**, 455 (2010).
16. B. R. Li, Y. J. Hsieh, Y. X. Chen, Y. T. Chung, C. Y. Pan, and Y. T. Chen, *J. Am. Chem. Soc.*, **135**, 16034 (2013).
17. F. Patolsky, G. Zheng, and C. M. Lieber, *Nat. Protoc.*, **1**, 1711 (2006).
18. Z. Fan, J. C. Ho, Z. a Jacobson, R. Yerushalmi, R. L. Alley, H. Razavi, and A. Javey, *Nano Lett.*, **8**, 20 (2008).
19. P. N. Brown, M. A. A. Mathews, L. A. Joss, C. P. Hill, and D. F. Blair, *J. Bacteriol.*, **187**, 2890 (2005).
20. F. N. Ishikawa, M. Curreli, H. K. Chang, P. C. Chen, R. Zhang, R. J. Cote, M. E. Thompson, and C. Zhou, *ACS Nano*, **3**(12), 3969 (2009).